IPNO DR 02-002

RELEASE PROPERTIES OF UC$_x$ AND MOLTEN U TARGETS

B. Roussière, F. Ibrahim, J. Sauvage, O. Bajeat, N. Barré,
F. Clapier, E. Cottereau, C. Donzaud, M. Ducourtieux,
S. Essabaa, D. Guillemaud-Mueller, C. Lau, H. Lefort,
C.F. Liang, F. Le Blanc, A.C. Mueller, J. Obert, N. Pauwels,
J.C. Potier, F. Pougheon, J. Proust, O. Sorlin, D. Verney
and A. Wojtasiewicz

Release properties of UC$_x$ and molten U targets

B. Roussière[1], F. Ibrahim[1], J. Sauvage[1], O. Bajeat[1], N. Barré[1], F. Clapier[1],
E. Cottereau[1], C. Donzaud[1], M. Ducourtieux[1], S. Essabaa[1], D. Guillemaud-Mueller[1],
C. Lau[1], H. Lefort[1], C.F. Liang[2], F. Le Blanc[1], A.C. Mueller[1], J. Obert[1], N. Pauwels[1],
J.C. Potier[1], F. Pougheon[1], J. Proust[1], O. Sorlin[1], D. Verney[1] and A. Wojtasiewicz[3]

[1] *Institut de Physique Nucléaire, F-91406 Orsay Cedex, France*
[2] *Centre de Spectrométrie Nucléaire et de Spectrométrie de Masse, F-91405 Orsay Cedex, France*
[3] *Warsaw University, 00-0681 Warsaw, Poland*

Abstract

The release properties of UC$_x$ and molten U thick targets associated with a Nier-Bernas ion source have been studied. Two experimental methods are used to extract the release time. Results are presented and discussed for Kr, Cd, I and Xe.

1   Introduction

At present time, two basic and complementary methods exist to produce high intensity radioactive nuclear beams: the in-flight method [1] which provides energetic fragments and the ISOL (Isotope Separation On-Line) method [2] which provides low-energy beams. For any ISOL type facility, a powerful method to produce neutron-rich nuclei is to use the fission mechanism induced by thermal neutrons, fast neutrons, high-energy protons or photons.

The research and development program PARRNe (Production d'Atomes Radioactifs Riches en Neutrons), developed at the Institut de Physique Nucléaire (IPN) at Orsay, is devoted to the study of the production of neutron-rich fission fragment beams extracted from thick targets [3]. An on-line isotope separator (PARRNe2), which is partly dedicated to the development of target and ion-source systems, has been installed at the Orsay tandem. The crucial point, when short-lived isotopes are produced in thick targets, is to build target and ion-source systems with good release properties and high efficiency.

The physical processes involved in the release of an atom are the diffusion in the target material, the desorption from the material surface and the effusion to the ion source outlet. The relative importance of these processes depends on the nature of the targets as well as on the chemical and physical properties of the elements to be released with regard to the surrounding materials. For example, it has been shown [4] that, at 1500°C for a target consisting of uranium oxide/carbide on a graphite cloth, the predominant release mechanism is desorption in the case of iodine and cesium, and diffusion in the case of xenon. The characterization of all these processes and their interplay are essential to define the targets needed for the radioactive nuclear beam projects. For solid targets,

various experimental and theoretical results are available [4-15]. Tests have been proposed to determine the predominant release process. In case one of the phenomena, diffusion, desorption or effusion is the time-controlling release mechanism, analytic expressions have been obtained for the release efficiency and for the release function which is the probability for an atom of a given element generated at t=0 to be released at time t. These analytic expressions depend on a release parameter that has been measured for some elements and for different target geometries. For molten targets, experimental data are much scarcer. The release of an atom seems to be governed mainly by the evaporation process provided that the surface of the target is pure and the diffusion in the target is fast enough [10]. It has been found that the release function can be written to a good approximation as a single exponential function [5, 10, 16] governed by one parameter, the release constant λ_R. This constant can be associated to a release time $T_R = \dfrac{\ln 2}{\lambda_R}$ defined as the time necessary for half the products created at $t = 0$ to escape from the target.

In this paper, we present the first results obtained with both an UC_x target and a molten U target, coupled to a Nier-Bernas ion source, with an emphasis on the analysis of the release properties of the targets for Kr, Cd, I and Xe. Firstly we describe the experiment and then the two methods used to obtain the release time: *i)* the direct measurement and *ii)* the determination from the comparison between the yields measured after separation and the yields in the target estimated from the fission cross-sections. Finally the results are discussed and compared to data available in the literature.

2 Description of the experiment

The 25 MeV deuteron beam delivered by the 15 MV tandem in Orsay [17] hits a 12 mm thick graphite converter placed 40 mm upstream from the center of the target. The fast neutrons produced in the break up of the deuterons irradiate the UC_x or molten U target. The UC_x target is composed of 64 disks of UC_x of 14 mm diameter and 1 mm thickness and contains 33 g of ^{238}U. These disks are placed in a graphite vessel and the whole is heated in a graphite oven up to 2200°C.

The overall dimensions of the molten U target are similar to those of the UC_x target. But due to the difference in density between molten U (16.3 g/cm^3 at 1700°C) and UC_x (3.3 g/cm^3), the molten U target contains much more ^{238}U than the UC_x target: 243 g instead of 33 g. Because molten U is very corrosive, a specific research and development study and numerous off-line tests were needed to choose the crucible [18]. Finally an Y_2O_3 one was adopted allowing the molten U target to be heated up to 1700°C during the experiment.

The fission fragments released from the target flow to the ion source through a 24 cm long and 1 cm diameter tantalum transfer line which can be heated up to 1700°C to reduce adsorption losses on the walls. Then they are ionized in a Nier-Bernas source [19]. The ions are extracted under 30 kV then mass separated by a magnet and finally collected on a mylar/aluminium tape in front of a Ge(HP) detector (energy resolution 1.9 keV at 1.3 MeV and efficiency 18%) in order to perform γ-spectroscopy measurements. Thus yields can be precisely determined for isobars and isotopes.

A new data acquisition system developed at IPN Orsay was used. It is based on a

COMET-6X (COdage et Marquage En Temps) module that allows us to encode in amplitude the signals delivered by up to six independent detectors and to associate with each amplitude encoding an absolute and high-resolution (400ps) time information. Thus using this module it is possible, with only one data taking, to perform various classical γ-spectroscopy measurements: singles γ-ray spectra, γ-γ-t coincidence and half-life determination. In the present work, we have used the singles γ-ray spectra to determine the yields and the correlated energy and time events to study the release properties of the targets.

3 Measurements

3.1 Direct measurements of the release time

The measurements have been performed as follows. The ion beam gate located in the mass-separated beam line is held in the opened position all through the measurement. From t = 0 to t_{irrad} the deuteron beam impinges on the converter and neutrons irradiate the target. From t = 0 to $t_{counting}$ the ions are collected on the tape in front of the germanium detector and the resulting activity is measured.

Since each γ energy is stored along with its associated absolute time on a DLT tape, the time step that appears the most convenient for the determination of the release time can be chosen off-line, in the course of the data analysis. This time step mainly depends on the statistics obtained and on the half-life of the nucleus on which the release-time measurement is performed. In the off-line treatment, we sorted the data in an E_γ-t bidimensional matrix, then we extracted the time spectra associated with the energy of the γ-rays corresponding to the decay of the nucleus, the release time of which is to be determined. Such spectra show the variation of the intensity of a given γ-ray versus time: each channel represents a time interval $\Delta t = t_2 - t_1$ and its content is proportional to the number of nuclei that decays between t_1 and t_2 ($N_d(t_1,t_2)$).

For molten targets as indicated above, the release function can be described to good approximation by a single exponential function. This approximation is also valid for solid targets if effusion or desorption is the predominant release mechanism [9]. In these cases, the analytic formula for $N_d(t_1,t_2)$ is easy to establish. Indeed, if Φ is the production rate in atoms/s for the nucleus of interest, and if the contribution of the parent can be neglected[1], the variation of the number of these nuclei in the target at the time t can be written as follows:

$$\frac{dN(t)}{dt} = \Phi - \lambda N(t) - \lambda_R N(t) \text{ for } 0 \leq t \leq t_{irrad}, \qquad (1)$$

$$\text{and } \frac{dN(t)}{dt} = -\lambda N(t) - \lambda_R N(t) \text{ for } t \geq t_{irrad}, \qquad (2)$$

where λ is the radioactive decay constant for the considered nuclei and λ_R the release constant associated with this element.

Then the number of nuclei present in the target at time t can be written as:

---

[1]This has been verified a posteriori: the γ-rays resulting from the parent decay are not significantly present in the spectra; moreover, in the A = 134 measurement performed to determine the release time of iodine, ^{134m}I is not fed by the Te decay.

$$N(t) = \frac{\Phi}{\lambda + \lambda_R} \left(1 - e^{-(\lambda + \lambda_R)t}\right) \text{ for } 0 \leq t \leq t_{irrad}, \qquad (3)$$

$$\text{and } N(t) = \frac{\Phi}{\lambda + \lambda_R} \left(e^{(\lambda + \lambda_R)t_{irrad}} - 1\right) e^{-(\lambda + \lambda_R)t} \text{ for } t \geq t_{irrad}. \qquad (4)$$

The variation of the number of nuclei present on the tape at time t, $N_1(t)$, can be written:

$$\frac{dN_1(t)}{dt} = \lambda_R \varepsilon_S N(t) - \lambda N_1(t),$$

with ε_S the overall efficiency of the separator including the ion-source efficiency and the transmission of the separator. Then the number of decays measured between t_1 and t_2 can be expressed as $N_d(t_1, t_2) = \int_{t_1}^{t_2} \lambda N_1(t) dt$, which gives:

$$N_d(t_1, t_2) = \frac{\varepsilon_S \Phi}{\lambda} \left(e^{-\lambda t_2} - e^{-\lambda t_1}\right) + \frac{\lambda_R \varepsilon_S \Phi}{\lambda + \lambda_R} (t_2 - t_1) - \frac{\lambda \varepsilon_S \Phi}{(\lambda + \lambda_R)^2} \left(e^{-(\lambda + \lambda_R)t_2} - e^{-(\lambda + \lambda_R)t_1}\right)$$

for $0 \leq t_1 \leq t_2 \leq t_{irrad}$ $\qquad (5)$, and

$$N_d(t_1, t_2) = \frac{\lambda \varepsilon_S \Phi}{(\lambda + \lambda_R)^2} \left(e^{(\lambda + \lambda_R)t_{irrad}} - 1\right) \left(e^{-(\lambda + \lambda_R)t_2} - e^{-(\lambda + \lambda_R)t_1}\right) - \frac{\varepsilon_S \Phi}{\lambda} \left(e^{\lambda t_{irrad}} - 1\right) \left(e^{-\lambda t_2} - e^{-\lambda t_1}\right)$$

for $t_{irrad} \leq t_1 \leq t_2$ $\qquad (6)$.

These final expressions are used to fit the experimental time spectra taking as free parameters, λ_R and a quantity proportional to $\varepsilon_S \Phi$.

3.1.1 Results with the UC_x target

The first test with the UC_x target was carried out at a target temperature of 2000 or 2200°C and a cold transfer line. The experimental conditions were not optimal during this measurement because of the failure of the heating system of the transfer line and the bad alignment between the deuteron beam and the converter. Figure 1 shows the time spectrum obtained for the the main γ-ray ($E_\gamma = 220.9$ keV and $I_\gamma = 20.1$ %) belonging to the ^{89}Kr ($T_{1/2} = 3.15$ m) decay, using the following experimental conditions: $T_{target} = 2000^oC$, $t_{irrad} = 912$ s and $t_{counting} = 1800$ s. The Kr release time is determined to be equal to 11.5 s. Another measurement performed on ^{90}Kr ($T_{1/2} = 32.3$ s) with $t_{irrad} = 200$ s and $t_{counting} = 500$ s leads to a Kr release time equal to 3.6 s for the UC_x target at 2200°C. The analysis of the measurements performed on ^{89}Kr and ^{90}Kr leads to T_R values which are different. The target temperature was not the same during both measurements, this can play a great part in the T_R change observed. However, although the fits obtained are of good quality, we cannot state that the expressions (5) and (6) given for $N_d(t_1, t_2)$ are the only ones suited to fit the experimental curves since the time-controlling release mechanism expected for a noble gas is diffusion rather than effusion. This point will be discussed further in section 3.2.2.

3.1.2 Results with the molten U target

Release-time measurements with the molten U target were performed on several isotopes having a half-life equal to about three minutes: ^{89}Kr ($T_{1/2} = 3.15$ m), ^{137}Xe ($T_{1/2} = 3.82$ m), ^{119}Cd ($T_{1/2} = 2.69$ m) and ^{134m}I ($T_{1/2} = 3.6$ m). The same irradiation and counting times were chosen for the four measurements: $t_{irrad} = 900$ s and $t_{counting} = 1800$ s. In each case, the target temperature was 1640°C and that of the transfer line, for a point located midway from the target and the ion source, was 1450°C for Kr and Xe and 1700°C for Cd and I. Figure 2 represents the time spectra obtained for the main γ-rays belonging

to the ^{89}Kr, ^{137}Xe, ^{119}Cd and ^{134m}I decays. The release times obtained fitting these data are: $T_R(Kr) = 72$ s, $T_R(Xe) = 112$ s, $T_R(Cd) = 180$ s and $T_R(I) = 1400$ s. The determination of the error on the measurements is quite difficult: two parameters are used to perform the fit, the first one (the release time) has an influence on the shape of the curve, and the second one (the quantity proportional to $\varepsilon_S \Phi$) is a scale factor. In order to study the interplay between these two parameters, we have performed various fits of each curve, fixing the release time and keeping the scale factor as the only free parameter. The results obtained using this procedure are given in figure 3 for ^{137}Xe. One can see that, when T_R is increased or decreased by a factor of 36%, the curve corresponding to the resulting fit is located at the upper or lower border of the experimental data. Applying this procedure to ^{89}Kr, ^{119}Cd and ^{134m}I, we have found the borderline fits for release times differing from T_R (the release time values indicated above) by a factor $\leqslant 50\%$. Thus in table 2, we have adopted 50% as a rough estimate of the T_R errors.

3.2 Determination of the release time from the comparison of the yields after separation with the yields expected in the target

The relevant quantity for the physicists interested in using radioactive beams is not the yield in the target but the yield available at the measurement point. For a given isotope, the number of ions collected per second on the tape, Φ_T, can be written as a function of Φ the number of atoms per second produced in the target, ε_S the overall efficiency of the separator, and ε_R the release efficiency: $\Phi_T = \varepsilon_S \ \varepsilon_R \ \Phi$.

Unlike what happens during the release-time measurements, the deuteron beam is permanently applied on the converter during the yield measurements, then an equilibrium is obtained in the target. In the frame of the previous approach used to describe the release of atoms from a molten target, the number of atoms of interest that remains present at any time t in the target written as $N(t) = \dfrac{\Phi}{\lambda + \lambda_R} \left(1 - e^{-(\lambda + \lambda_R)t} \right)$ can be approximated by $\dfrac{\Phi}{\lambda + \lambda_R}$. λ_R being the release probability, Φ_T can be written $\varepsilon_S \ \lambda_R \ \dfrac{\Phi}{\lambda + \lambda_R}$. Thus, as mentioned in refs.[4, 20, 21], for molten targets the release efficiency is defined by:

$$\varepsilon_R = \frac{\lambda_R}{\lambda + \lambda_R} = \frac{T_{1/2}}{T_{1/2} + T_R} \qquad (7).$$

For solid targets, different formulas for the release efficiency have been established depending on whether the predominant release process is diffusion, desorption or effusion [4, 9]. These formulas are written as a function of a release or delay parameter, often called μ or ν in case of diffusion or desorption and effusion, respectively. By analogy with the notations used for the molten targets, we define a release time T_R by $T_R = \dfrac{\ln 2}{\mu}$ or $\dfrac{\ln 2}{\nu}$. It is worth noting that, except in the case of diffusion, this release time has a very simple meaning. It is called half-time for release in ref. [7] and represents the time necessary before half the amount produced at a certain moment has been released. The

release efficiency can then be written as a function of T_R:

$$\varepsilon_R = \frac{T_{1/2}}{T_{1/2} + T_R} \quad \text{in case of effusion or desorption} \qquad (8),$$

$$\varepsilon_R = \frac{3(\sqrt{\pi^2 T_R/T_{1/2}} \, \coth(\sqrt{\pi^2 T_R/T_{1/2}}) \, - \, 1)}{\pi^2 T_R/T_{1/2}} \quad \text{in case of radial diffusion in spherical}$$

grains $\qquad$ (9),

$$\varepsilon_R = \frac{\tanh(\sqrt{\pi^2 T_R/4T_{1/2}})}{\sqrt{\pi^2 T_R/4T_{1/2}}} \quad \text{in case of diffusion in an infinite foil} \qquad (10).$$

Figure 4 shows the release efficiency ε_R as a function of $T_R/T_{1/2}$. In all cases, the release efficiency remains equal to 1 for $T_R < 0.01 \times T_{1/2}$ and the various curves begin to show appreciable changes when $T_R > 5 \times T_{1/2}$. In particular, in a log-log diagram as in fig. 4, the asymptotic slope is equal to -1 for molten target and for solid target in case of desorption or effusion and -0.5 for solid target in case of diffusion.

Through an isotopic series, T_R is constant, therefore ε_R only depends on the half-life of each isotope according to the relations (7-10). Provided the Φ_T and Φ values for various isotopes are known, the ratio $\dfrac{\Phi_T}{\Phi} = \varepsilon_S \varepsilon_R$ can then be plotted versus $\dfrac{1}{T_{1/2}}$. Since ε_S is also constant through an isotopic series, we can determine the predominant release process from the asymptotic behaviour of $\dfrac{\Phi_T}{\Phi}$. Finally, to determine the ε_S and T_R values, the quantity $\varepsilon_S \varepsilon_R$, where ε_R is described by one of the relations (7-10), is used to fit the $\dfrac{\Phi_T}{\Phi}$ data.

The question now is to evaluate Φ_T and Φ. The Φ_T values for Kr, Cd, I and Xe isotopes have been measured [22] and are presented in table 1.

The number of fissions induced in both targets (N_f) was estimated using the code developed by M. Mirea *et al.* [23] which takes into account the converter material, the energy of the incident deuterons, the angular and energy distributions of the emergent neutrons and the geometry of the converter-target system. With an 1 μA 25 MeV incident deuteron beam, a total of 2.5×10^8 and 1.5×10^9 fissions per second was calculated for the UC$_x$ and molten U targets, respectively [24]. Then the Φ values can be estimated provided the fission product yields per 100 fissions (Y) are known: $\Phi = N_f \times \dfrac{Y}{100}$. With an incident 25 MeV deuteron beam, the energy distribution of the neutrons at $0°$ is characterized by a mean energy of 10 MeV and a full width at half maximum of around 10 MeV [25]. To our knowledge, the fission product yields per fission are not available for these neutron energies. In the following analysis, we have used, among the sets of recommended cumulative yields given by T.R. England and B.F. Rider [26], the set corresponding to the energies of the neutron spectrum produced by fission and that given for neutrons with 14.7 MeV energy, *i.e.* two data sets corresponding to neutron energies enclosing our experimental energy distribution. These cumulative yields are also indicated in table 1.

Table 1: Yields (in atoms/s) of Kr, Xe, Cd and I isotopes measured on the tape for the UC_x (T_{target} = 2000ºC and T_{line} = 1400ºC) and molten U (T_{target} = 1640ºC and T_{line} = 1450ºC) targets using a $1\mu A$ 25 MeV incident deuteron beam. The fission product yields per 100 fissions for ^{238}U are also indicated, they are labeled Y(F) for fission spectrum energies and Y(HE) for 14.7 MeV neutron energy [26].

Nuclei	$T_{1/2}$	$\Phi_T(UC_x)$ [a]	Φ_T(molten U) [a]	Y(F) [b]	Y(HE) [b]
^{87}Kr	1.27 h	2. 10^4	3.75 10^4	1.63	1.68
^{88}Kr	2.84 h	2. 10^4	3.75 10^4	2.03	2.16
^{89}Kr	3.15 m	3.5 10^4	5. 10^4	2.67	2.81
^{90}Kr	32.3 s	2.5 10^4	2.5 10^4	3.08	2.75
^{91}Kr	8.6 s	1.5 10^4	6.25 10^3	3.35	2.52
^{92}Kr	1.84 s	7. 10^3	1.75 10^3	2.65	1.66
^{93}Kr	1.29 s	3. 10^3	7.5 10^2	1.46	0.73
^{119}Cd	2.69 m	1.3 10^4	2.5 10^4	1.99 10^{-2}	3.63 10^{-1}
^{120}Cd	50.8 s	1.5 10^4	3.33 10^4	3.86 10^{-2}	7.74 10^{-1}
^{121}Cd	13.5 s	1.1 10^4	4.5 10^3	3.61 10^{-2}	8.17 10^{-1}
^{122}Cd	5.24 s	6. 10^3	3.75 10^3	3.72 10^{-2}	7.89 10^{-1}
^{123}Cd	2.1 s	7. 10^3	8.75 10^2	3.24 10^{-2}	7.39 10^{-1}
^{124}Cd	1.24 s	4. 10^3	3.75 10^2	2.20 10^{-2}	6.15 10^{-1}
^{132}I	2.28 h	8. 10^3	3. 10^4	5.15	4.84
^{133}I	20.8 h	3.5 10^4	5. 10^5	6.76	6.00
^{134}I	52.6 m	3. 10^4	5. 10^5	7.60	6.37
^{135}I	6.57 h	2.5 10^4	1. 10^6	6.94	5.50
^{136}I	83.4 s	5. 10^3	1.5 10^4	4.99	3.01
^{137}I	24.5 s	1. 10^3	6. 10^3	5.13	3.12
^{135}Xe	9.1 h	8.5 10^4	2.2 10^5	6.97	5.84
^{137}Xe	3.8 m	7. 10^4	2.5 10^5	6.04	4.72
^{138}Xe	14.0 m	8. 10^4	3. 10^5	5.70	4.53
^{139}Xe	39.7 s	6. 10^4	8. 10^4	5.32	3.39
^{140}Xe	13.6 s	2. 10^4	2. 10^4	4.90	2.74
^{141}Xe	1.7 s	1. 10^4	2.5 10^3	3.19	1.36

[a] uncertainty $\sim$ 50%

[b] uncertainty < 8% for Kr, > 45% for Cd, < 16% for I and < 6% for Xe

Table 2: T_R values obtained for Kr, Cd, I and Xe released by the molten U target. The overall efficiency of the separator is also indicated.

| | from the comparison with | | | | from the direct |
| | Y(F) | | Y(HE) | | measurements |
Element	T_R [s]	ε_S [%]	T_R [s]	ε_S [%]	T_R [s]
Kr	66±30	0.14±0.04	40±21	0.13±0.04	72±36
Cd	272±482	23±37	261±391	1.2±1.9	180±90
I	2202±1195	0.63±0.23	1474±814	0.7±0.25	1400±700
Xe	94±45	0.27±0.08	56±30	0.32±0.1	112±56

3.2.1 Results with the molten U target

Figure 5 represents the $\dfrac{\Phi_T}{\Phi}$ ($\dfrac{\Phi_T}{\Phi} = \varepsilon_S \varepsilon_R$) values as a function of $\dfrac{1}{T_{1/2}}$ for Kr, Cd, I and Xe. Except for one point corresponding to the ^{132}I data which seems to be inconsistent, these values exhibit the behaviour expected for the molten target, in particular the asymptotic slope equal to -1 in this log-log diagram. The curves drawn in figure 5 show the result of the fits obtained with ε_R defined by equation (7) for the T_R and ε_S parameter values listed in table 2. The T_R values obtained by the direct measurement of the release time presented in section 3.1 are also reported in table 2. We can note that both methods give similar results. This shows that although the yields in the target are not precisely known, using the sets of fission product yields corresponding to neutron energies enclosing our experimental distribution leads to reasonable estimates of the release time. The errors on T_R obtained by this second method are also of the order of 50%, except for Cd. In the Cd case, no experimental Φ_T values are available for isotopes with $T_{1/2} > T_R$ (see tables 1 and 2), so the plateau expected in the $\dfrac{\Phi_T}{\Phi}$ curve for the low values of $\dfrac{1}{T_{1/2}}$ is not accurately defined. Consequently the errors on ε_S as well as the errors on T_R are high. The ε_S values of the overall efficiency of the separator obtained from the analysis using Y(HE) or Y(F) are quite similar except for Cd for which the yields are very sensitive to the energy of the neutron inducing fission.

3.2.2 Results with the UC$_x$ target

Figure 6 shows the $\dfrac{\Phi_T}{\Phi}$ ($\dfrac{\Phi_T}{\Phi} = \varepsilon_S \varepsilon_R$) values as a function of $\dfrac{1}{T_{1/2}}$ for Kr, Cd, I and Xe. For iodine, the data displayed in fig. 6 indicate clearly an asymptotic slope equal to -1. This means that the dominant release process is effusion or desorption. For Kr, Cd and Xe, although Φ_T has been measured for isotopes with short half-lives ($T_{1/2} \sim$ 1s), it is not obvious from fig. 6 that the $\dfrac{\Phi_T}{\Phi}$ asymptotic behaviour is reached. This shows the limits of the method. In order to define the dominant release process, the $\dfrac{\Phi_T}{\Phi}$ asymptotic behaviour is needed. When T_R is short, yield determination for isotopes with very short half-lives is necessary. But for such exotic isotopes, spectroscopic information

Table 3: T_R values obtained for Kr, Cd, I and Xe released by the UC_x target. The overall efficiency of the separator is also indicated.

| | | from the comparison with | | | |
| | | Y(F) | | Y(HE) | |
Element	Release mechanism	T_R [s]	ε_S [%]	T_R [s]	ε_S [%]
Kr	diffusion	30±8	0.46±0.12	8.3±3.3	0.44±0.10
Cd	diffusion	24±56	23±18	28±65	1.15±0.99
I	desorption or effusion	440±240	0.17±0.05	315±175	0.21±0.06
Xe	diffusion	52±30	0.52±0.17	15±13	0.62±0.22

such as absolute γ-intensities is not always available. For example, although the γ-rays corresponding to the ^{94}Kr decay have been clearly observed, the yield of ^{94}Kr could not be determined because, for the ^{94}Kr $\rightarrow$ ^{94}Rb decay, only the relative γ-intensities are known. For Cd, Kr and Xe, we have performed the analysis of the data assuming that the dominant release process is either diffusion or effusion, desorption. In all cases, the best fits have been obtained assuming diffusion. This agrees with what is expected for the Kr and Xe noble gases.

The curves drawn in fig. 6 show the result of the fits using ε_R defined by equations (8) and (9) for the ε_S and T_R parameter values listed in table 3. As expected, the release times obtained for Kr, Cd, I and Xe with the UC_x target are much shorter than the T_R values found with the molten U target. Concerning the overall efficiency of the separator, as already noticed with the molten U target, the two ε_S estimates extracted from the comparison of Φ_T with Y(HE) and Y(F) are very similar, except for Cd.

We have shown that the most probable release process for Kr is diffusion. This implies that the analytic expressions used for $N_d(t_1,t_2)$ to fit the data in the direct measurement of the release time (see section 3.1.1) are not valid for Kr released from an UC_x target. However, one can note that the T_R value obtained for ^{89}Kr ($T_{target} = 2000$°C) by the direct method lies between the values listed in table 3. For the special case $T_R \ll T_{1/2}$, the release efficiencies corresponding to diffusion or effusion are very close (see fig. 4). This is the case for ^{89}Kr since the $T_R/T_{1/2}$ values obtained from the release times listed in table 3 are small ($4.\times10^{-2} < T_R/T_{1/2} < 0.16$). On the other hand, we have plotted in figure 7 the release functions $P(t)\times e^{-\lambda t}$ for ^{89}Kr and different T_R values: 11s and 1890s. Using these release functions, we have calculated the number of disintegrations expected for the irradiation and counting conditions used during the direct measurement of the release time (see section 3.1). The corresponding simulated time spectra are also presented in figure 7 and can be directly compared to the experimental ones shown in figs. 1 and 2. When $T_R/T_{1/2} = 5.8 \ 10^{-2}$ (*i.e.* the value obtained in section 3.1.1 for ^{89}Kr released from the UC_x target), the release function obtained for diffusion differs from the single exponential function used for effusion or for molten target only for the very low t values (fig. 7a), and the time spectra obtained for diffusion or effusion are identical (fig. 7c). On the contrary, when $T_R/T_{1/2} = 10$, the release functions obtained for diffusion or effusion are quite different (fig. 7b), and consequently the shape obtained for the time spectra (fig. 7d). All these facts allow us to understand why, in the analysis of Kr released from the UC_x target presented in section 3.1.1, the use of the analytic expressions of $N_d(t_1,t_2)$

given in equations (5) and (6), even though inappropriate, led to a realistic estimate of T_R.

4   Discussion

In this section, we will compare our release time and overall efficiency results with the data available in the literature. This discussion will be rather qualitative because *i)* the accuracy on the T_R determination is not high, *ii)* the T_R and ε_S values depend strongly on the experimental conditions (temperature, geometry and nature of the target, temperature of the transfer line, type and parameters of the ion source) and *iii)* little has been published on the Nier-Bernas ion-source efficiencies and on release times for Kr, Cd, I and Xe.

The ε_S efficiency values obtained for each element are rather similar in both experiments. For Kr, I and Xe they are a little less than one per cent, fitting rather well with what can be expected for our Nier-Bernas ion source. Indeed, during these experiments, the efficiencies have been measured on stable isotopes using a calibrated leak, they were found lying in the range [0.1-0.5%] for Kr and [0.3-0.6%] for Xe. Such efficiencies can look low but Kr and Xe are noble gases and difficult to ionize with this type of ion source. Moreover an ion source has to be optimized for each element or group of elements. For example the alkali, alkali-earth and rare earth elements are efficiently ionized ($\varepsilon_S > 50\%$) by means of surface ionization sources, and most of the elements seem ionizable ($\varepsilon_S > 1\%$) by means of plasma-discharge sources working at high temperature [27]. For Cd isotopes, depending on the set of fission yields (Y(HE) or Y(F)) used for the T_R and ε_S estimates, the efficiency varies from $\sim 1\%$ up to 24%. Such values seem realistic since efficiencies up to 36% for Cd have been obtained with a Nier-Bernas source [28].

To our knowledge, nothing has been published in the literature about the release times of Kr, Cd and I in the case of molten targets and the behaviour of Xe has only been studied using a molten La target. In ref. [10], the delay time for Xe in a molten La target at 1200°C is reported to be $\tau = 24$ s, which corresponds to $T_R = 16.6$ s, taking into account the relation between τ and T_R ($T_R = \tau \times \ln 2$). This latter value has to be compared to our result: $T_R = 112$ s for Xe in a molten U target at 1640°C. At first sight, our release-time estimate appears to be much longer than that given with the molten La target. However, it has been shown [10] that, for volatile products like Xe, the determining release process is no longer evaporation but diffusion through the liquid. In this case, the release time of a given element from a molten target depends strongly on the ratio V_0/S_0, where V_0 is the volume of the target and S_0 its surface: the measurements for Rb reported in ref. [10] indicate that T_R is directly proportional to V_0/S_0. The $T_R = 16.6$ s value for Xe was measured for a target with $V_0 = 15$ cm^3 and $S_0 = 60$ cm^2, which implies V_0/S_0 = 0.25 cm. In our case the characteristics of the target were $V_0 = 14.9$ cm^3 and $S_0 = 9.34$ cm^2, which gives $V_0/S_0 = 1.59$ cm. These ratios have to be corrected for the density of the two different target materials, thus $V_0/S_0 = 1.54$ g/cm^2 for the La target and 25.9 g/cm^2 for the U target. One would expect $T_R \sim 280$ s for Xe in the molten U target. The difference between this estimate and our experimental value ($T_R = 112$ s) can be due to the temperature of the targets. Indeed, the experiment with the molten La target was performed at ~ 300°C above the melting point and our experiment with U took place at

11

Table 4: Release of UC_x targets

Element	T_{target} = 2000°C present work		T_{target} = 1500°C refs. [4, 7]		T_{target} =2400°C ref. [7]	
	Mechanism	T_R [s]$^{a)}$	Mechanism	T_R [s]	Mechanism	T_R [s]
Kr	diffusion	8.3 or 30		100	diffusion	1.0
Cd	diffusion	28 or 24		11	desorption	1.5
I	desorption or effusion	315 or 440	desorption	30	desorption	0.14
Xe	diffusion	15 or 52	diffusion	270	diffusion	15

a) obtained from the comparison between the yields measured after separation and the yields in the target estimated from the fission cross-sections (see table 3).

$\sim$ 500°C above the melting point.

The release times we obtained with the UC_x target can be compared to previous results since the production of neutron rich nuclei obtained by fission has been carried out systematically at the OSIRIS facility [7, 8]. Table 4 gives a comparison between the release times obtained in the present work and those reported in refs. [4, 7]. The release mechanism, when available, is also indicated. One can note that, for Kr and Xe, our results measured with a target at 2000°C lie between the values found at 1500° and 2400°C, which confirms the great dependence of T_R upon the temperature of the target. For Cd, we obtain at 2000°C a release time longer than that given at 1500°C, which is unexpected. We can note that, whereas diffusion seems to be the time-controlling mechanism for Cd at 2000°C, desorption has been assumed at 2400°C [7]. If we analyse our Cd data assuming effusion or desorption, then the release time is found to be $\sim$ 2 s, in quite good agreement with the results of ref. [7], but in this case the quality of the fit is poor. For iodine, the release time found in our experiment with the UC_x target is much longer than the values obtained in the OSIRIS experiment. Both methods that we have used to determine T_R for the molten U target gave similar results and long values for iodine. This gives confidence in the release-time value obtained for iodine using the UC_x target. An important contribution to T_R could come from losses elsewhere in the target ion-source system and not only from the release from the target. For instance, as the tantalum transfer line shows a temperature gradient, the iodine atoms could be trapped in the coldest point. Moreover the chemical affinity between tantalum and iodine could also explain the long iodine release times that we have measured. Both phenomena are avoided in the OSIRIS set-up: the target is integrated into the ion source giving a strong thermal coupling between both elements and no element of the target ion-source system is made of tantalum.

5 Conclusions

In the frame of the approach describing the release of nuclei from a molten target, two experimental methods have been used to extract the release time associated with various elements: Kr, Cd, I and Xe. It has been shown that both methods give similar results. The release of these elements from an UC_x target has been also investigated. The values obtained for the release time are in good agreement with the data available in the literature, except for iodine. It appears also that, when the yields per fission are known even

roughly for a given element, the measurement of the yields after separation for only a few masses of an isotopic series, but including long and short half-lives, allows: *i)* the determination of the predominant release process and *ii)* the estimate of the release time and of the overall efficiency of the separator. As the release times and the ion-source efficiencies are crucial points for the design of high intensity nuclear beam facilities, it is of great interest to extend this work to other elements and ion sources. In this respect, we have started a release-time measurement program using an UC_x target with a hot plasma MK5-ISOLDE-type ion source [29] designed for the ionization of not very volatile elements like those of groups Ib, III, IV and V. However, we have already obtained experimental data that support fast neutrons to be a powerful means of producing high intensity neutron-rich radioactive nuclear beams. Indeed, the number of fission fragments that we observed, *i.e.* released from the target and ionized, fits rather well with what could be expected from the target and ion-source system used. This gives confidence in the extrapolations made for the future high intensity facilities, provided that the converter and the target can withstand the heat brought respectively by an intense incident beam and the fission itself.

References

[1] A.C. Mueller and B.M. Sherrill, Annu. Rev. Nucl. Part. Sci. **43** (1993) 529.

[2] H.L. Ravn, Nucl. Instr. and Meth. **B 26** (1987) 72.

[3] F. Clapier *et al.*, Phys. Rev. ST-AB **1** (1998) 013501.

[4] G. Rudstam, Nucl. Instr. and Meth. **A 256** (1987) 465.

[5] L.C. Carraz *et al.*, Nucl. Instr. and Meth. **148** (1978) 217.

[6] L.C. Carraz *et al.*, Nucl. Instr. and Meth. **158** (1979) 69.

[7] G. Rudstam *et al.*, Radiochimica Acta **49** (1990) 155.

[8] B. Fogelberg *et al.*, Nucl. Instr. and Meth. **B 70** (1992) 137.

[9] R. Kirchner, Nucl. Instr. and Meth. **B 70** (1992) 186.

[10] H.L. Ravn, Physics Reports **54** (1979) 201.

[11] A.H.M. Evensen *et al.*, Nucl. Instr. and Meth. **B 126** (1997) 160.

[12] A.E. Barzakh *et al.*, Nucl. Instr. and Meth. **B 126** (1997) 150.

[13] J.R.J. Bennett, Nucl. Instr. and Meth. **B 126** (1997) 146.

[14] J. Lettry *et al.*, Nucl. Instr. and Meth. **B 126** (1997) 130.

[15] C.J. Densham *et al.*, Nucl. Instr. and Meth. **B 126** (1997)154.

[16] H.L. Ravn, Nucl. Instr. and Meth. **139** (1976) 281.

[17] B. Waast *et al.*, Nucl. Instr. and Meth. **A 287** (1990) 26.

[18] S. Kandri-Rody *et al.*, Nucl. Instr. and Meth. **B 160** (2000) 1.

[19] I. Chavet and R. Bernas, Nucl. Instr. and Meth. **51** (1967) 77.

[20] H.L. Ravn, S. Sundell, L. Westgaard and E. Roeckl, J. Inorg. Nucl. Chem. **37** (1975) 383.

[21] B. Roussière, Thèse de 3eme cycle, Université Paris VI, IPNO-T-81-05.

[22] F. Ibrahim *et al.*, to be published.

[23] M. Mirea *et al.*, Rapport Interne IPNO 99-06 (1999).

[24] O. Bajeat, private communication.

[25] S. Ménard *et al.*, Phys. Rev. Spec. Top.-AB vol. 2 (1999) 033501.

[26] R.T England and B.F. Rider, Los Alamos Laboratory report LA-UR-94-3106, *http://t2.lanl.gov/publications/yields/.*

[27] H.L. Ravn *et al.*, Nucl. Instr. and Meth. **B 88** (1994) 441.

[28] G. Lempert and I. Chavet, Nucl. Instr. and Meth. **139** (1976) 7.

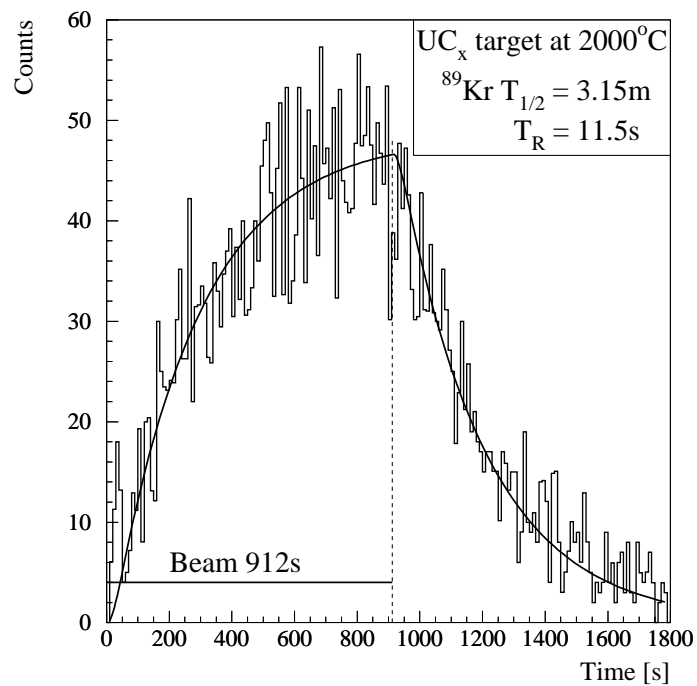[29] S. Sundell, H. Ravn and the ISOLDE collaboration, Nucl. Instr. and Meth. **B 70** (1992) 160.

Figure 1: Time spectrum for the 220.9 keV γ-line of the ^{89}Kr decay. Each point of the histogram corresponds to a 10 s time interval. The full line indicates the result of the fit for the T$_R$ value indicated in the inset.
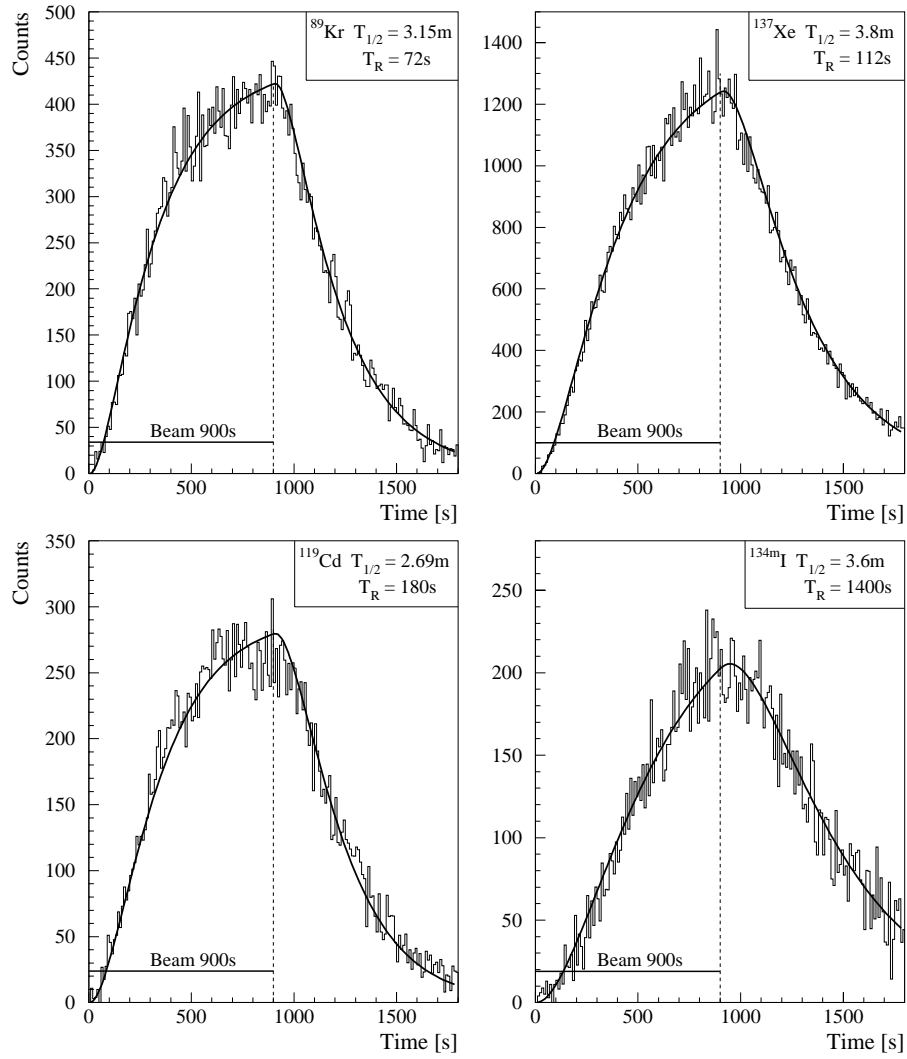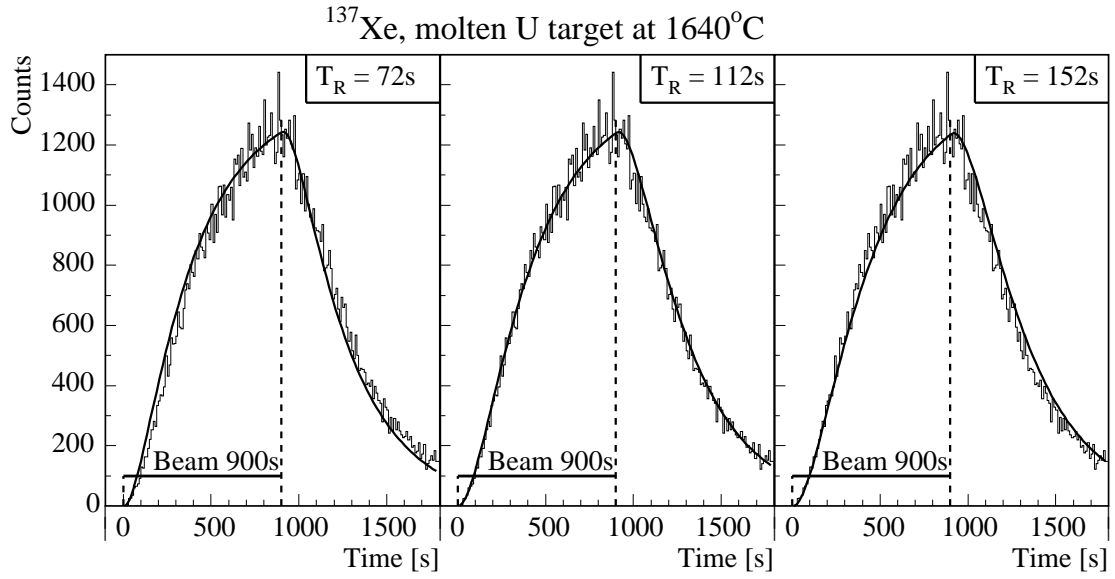
Figure 2: Time spectra for the main transitions of the ^{89}Kr, ^{137}Xe, ^{119}Cd and ^{134m}I decays. Each point of the histogram corresponds to a 10 s time interval. The full lines indicate the result of the fit for the T$_R$ values indicated in the insets.

Figure 3: Time spectrum for the main transition of the ^{137}Xe decay. Comparison between various fits obtained fixing the release time to the values indicated in the insets and keeping the scale factor as the only parameter.
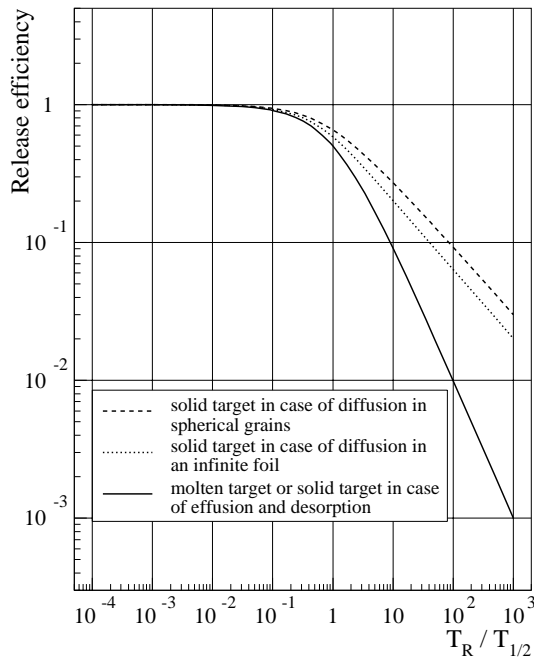

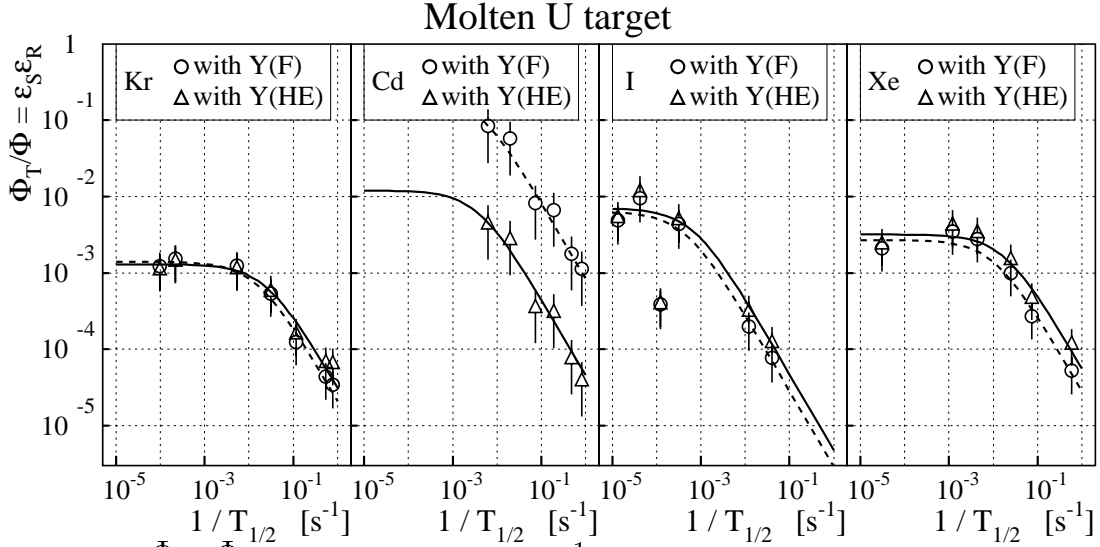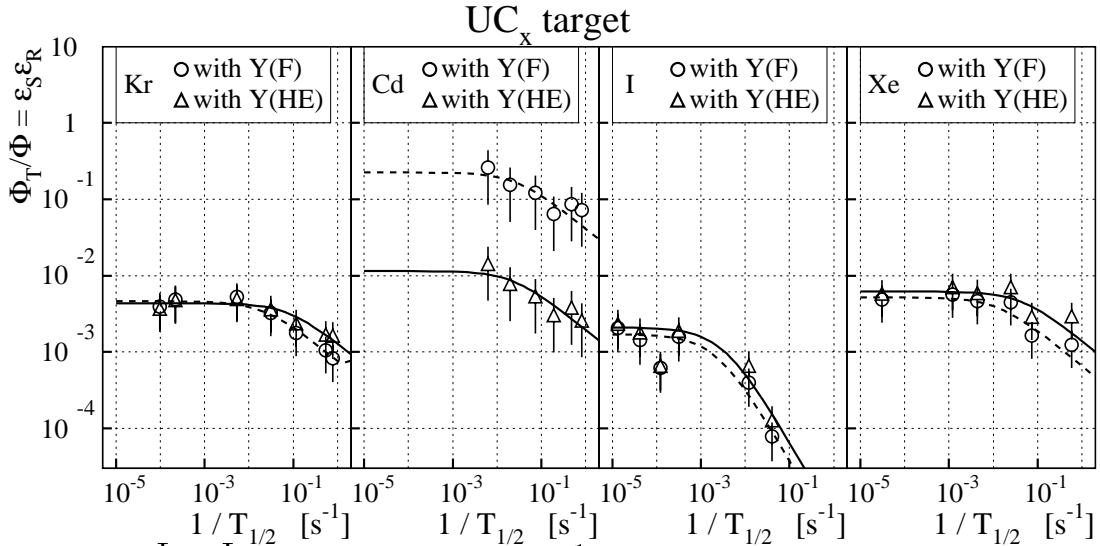Figure 4: Theoretical release efficiency for molten and solid targets.

Molten U target

Figure 5: The $\frac{\Phi_T}{\Phi}$ ($\frac{\Phi_T}{\Phi} = \varepsilon_S \varepsilon_R$) values versus $\frac{1}{T_{1/2}}$ for the Kr, Cd, I and Xe isotopes calculated using the Φ_T(molten U), Y(HE) and Y(F) values given in table 1. The solid (dashed) lines indicate the result of the fit of the data represented by $\triangle$ ($\bigcirc$).

UC$_x$ target

Figure 6: The $\frac{\Phi_T}{\Phi}$ ($\frac{\Phi_T}{\Phi} = \varepsilon_S \varepsilon_R$) values versus $\frac{1}{T_{1/2}}$ for the Kr, Cd, I and Xe isotopes calculated using the Φ_T(molten U), Y(HE) and Y(F) values given in table 1. The solid (dashed) lines indicate the result of the fit of the data represented by $\triangle$ ($\bigcirc$).
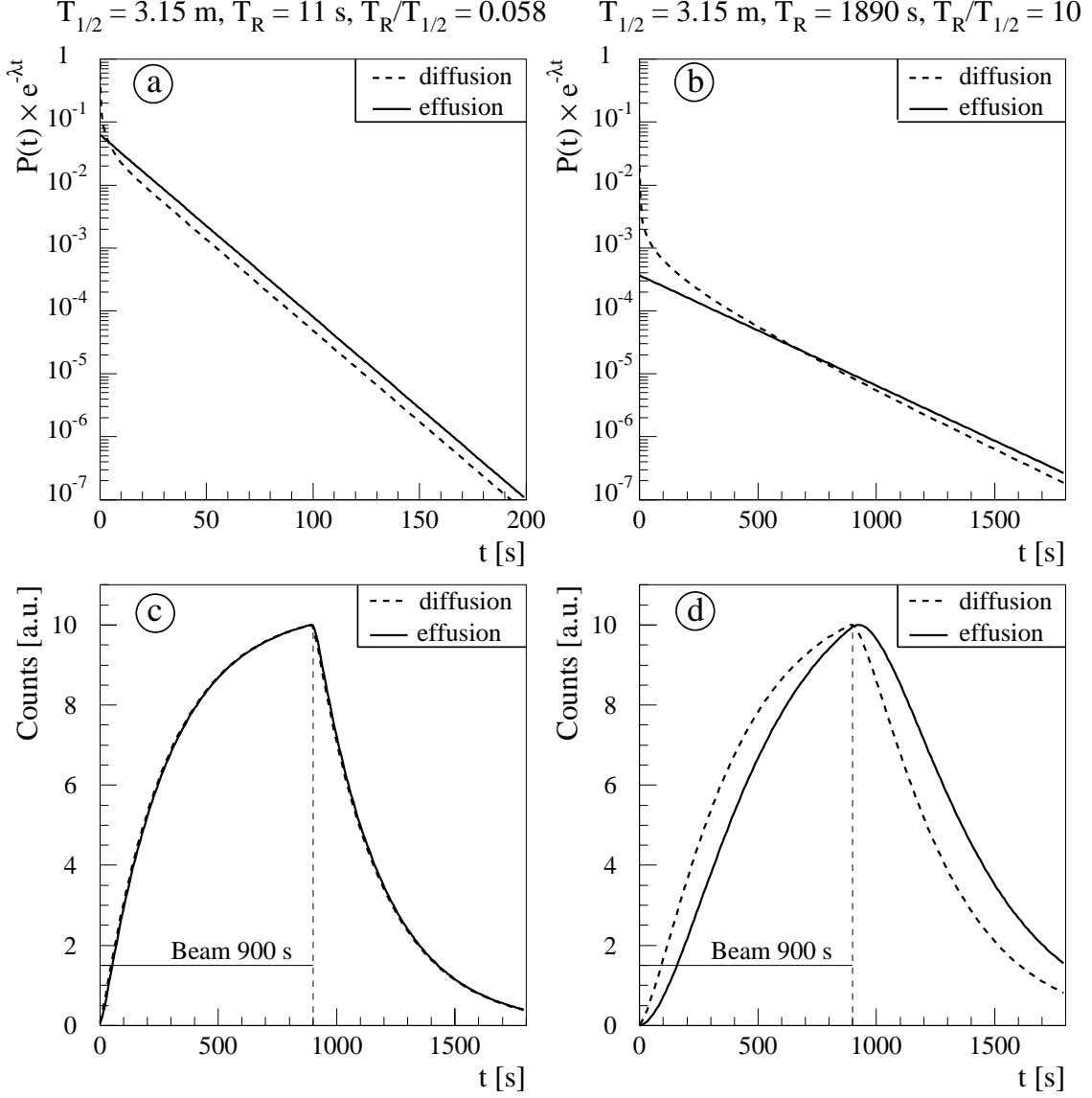
Figure 7: a) and b) Release functions calculated for ^{89}Kr using $T_R = 11$ s and $T_R = 1890$ s. $P(t)$ is defined by $\dfrac{6\mu_0}{\pi^2} \sum\limits_{k=1}^{\infty} e^{-k^2 \mu_0 t}$ with $\mu_0 = \dfrac{\ln 2}{T_R}$ in case of diffusion in spherical grains and $\nu e^{-\nu t}$ with $\nu = \dfrac{\ln 2}{T_R}$ in case of effusion.

c) and d) Time spectra calculated using these release functions and corresponding to the number of disintegrations expected per 10 s with a 900 s irradiation time and a 1800 s total counting time. Each spectrum is normalized so that its maximum is equal to 10.